20th Australasian Fluid Mechanics Conference
Perth, Australia
5-8 December 2016

Instabilities in the Wake of a Circular Cylinder with Near-wake Wire Disturbances

Hongyi Jiang[1], Liang Cheng[1,2] and Hongwei An[1]

[1]School of Civil, Environmental and Mining Engineering
The University of Western Australia, 35 Stirling Highway, Crawley, WA 6009, Australia

[2]State Key Laboratory of Coastal and Offshore Engineering
Dalian University of Technology, Dalian, 116024, China

Abstract

The secondary instabilities in the wake of a circular cylinder with near-wake wire disturbances are investigated by using three-dimensional (3D) direct numerical simulations (DNS). For one wire placed asymmetrical about the wake centreline and two wires placed symmetrical about the wake centreline, the secondary instabilities are found to be Mode C and Mode A, respectively. The existence of the Z_2 spatiotemporal symmetry in the two-dimensional (2D) wake flow of the two-wire scenario is responsible for the suppression of Mode C.

Introduction

The topic of three-dimensional (3D) instabilities in the wake of bluff bodies has received great attention during the past two decades due to its fundamental and practical significance. One of the most classical case is steady incoming flow past a long circular cylinder, for which the wake instabilities are governed by a single dimensionless parameter Re (= UD/ν), where U is the approaching flow velocity, D is the cylinder diameter, and ν is the fluid viscosity. It has been demonstrated (e.g., Williamson, 1996) that with the increase of Re, the wake flow undergoes a transition sequence of (1) emergence of primary wake instability at Re ~ 47, (2) onset of Mode A instability with large-scale vortex dislocations (i.e., Mode A*) at Re ~ 190, (3) gradual transition from Mode A* to Mode B over a range of Re from 230 to 260, and (4) development of increasingly disordered Mode B structure beyond Re ~ 270.

Based on a surge of studies in the recent years of 3D wake instabilities involving different bluff body configurations, arrangements or movements with respect to the classical case of an isolated stationary circular cylinder, a different wake instability mode, i.e., Mode C, has often been reported in the literature. As shown by Blackburn and Sheard (2010), the Mode C instability is triggered by a perturbation imposed on the bluff body which causes the breaking of the Z_2 spatiotemporal symmetry of the wake. Such perturbations can normally be bluff body configurations, arrangements or movements that are asymmetric about the wake centreline, e.g., a circular cylinder with a trip-wire in the near-wake but offset from the wake centreline (Zhang et al., 1995; Yildirim et al., 2013), a circular ring (Sheard et al., 2003), a rotated square cylinder (Sheard et al., 2009), two circular cylinders in staggered arrangements (Carmo et al., 2008), a rotating circular cylinder (Rao et al., 2013), etc.

In addition to the configuration of a circular cylinder with a trip-wire in the near-wake but offset from the wake centreline (referred to as the "one-wire scenario" hereafter), the numerical study by Zhang et al. (1995) also reported a Mode C instability for the configuration of a circular cylinder with two near-wake wires placed symmetrical about the wake centreline (referred to as the "two-wire scenario" hereafter). In the two-wire scenario, since the geometric configuration is symmetrical about the wake centreline, it is suspected that the wake flow may still possess a Z_2 spatiotemporal symmetry, which is not in line with the mechanism for Mode C instability proposed by Blackburn and Sheard (2010). Therefore, the secondary instability of the two-wire scenario warrants a re-visit, which forms the motivation of this study.

Numerical Model

Numerical Method

OpenFOAM (www.openfoam.org) has been adopted in solving the continuity and the incompressible Navier-Stokes equations:

$$\frac{\partial u_i}{\partial x_i} = 0 \tag{1}$$

$$\frac{\partial u_i}{\partial t} + u_j \frac{\partial u_i}{\partial x_j} = -\frac{1}{\rho}\frac{\partial p}{\partial x_i} + \nu \frac{\partial^2 u_i}{\partial x_j \partial x_j} \tag{2}$$

where $(x_1, x_2, x_3) = (x, y, z)$ are the Cartesian coordinates, u_i is the velocity component in the direction of x_i, t is the time, and p is the pressure. The FVM (Finite Volume Method) and the PISO (Pressure Implicit with Splitting of Operators) algorithm (Issa, 1986) are adopted for solving the equations. The convection, diffusion and time derivative terms are discretized, respectively, using a fourth-order cubic scheme, a second-order linear scheme, and a blended scheme consisting of the second-order Crank-Nicolson scheme and a first-order Euler implicit scheme, respectively. By using the same numerical formulation, Jiang et al. (2016) predicted wake transitions of flow past an isolated circular cylinder ($45 \leq Re \leq 300$) that are in good agreement with the experimental results reported by Williamson (1996).

Geometrical Configuration and Boundary Conditions

A hexahedral computational domain of $(L_x, L_y, L_z) = (50D, 40D, 12D)$ (L_x, L_y, and L_z being the domain sizes in the x-, y-, and z-directions, respectively), as shown in Figure 1(a), is adopted for the present DNS. For the one-wire scenario, a circular wire is placed in the near-wake of the main circular cylinder at $(x/D, y/D) = (0.75, 0.75)$ (Figure 1), to be consistent with the experimental and numerical setups in Zhang et al. (1995). The diameter of the wire, D_w, is chosen as $0.05D$, which is the same as that employed in the numerical study by Zhang et al. (1995). For the two-wire scenario, two circular wires with $D_w = 0.05D$ are placed at $(x/D, y/D) = (0.75, \pm 0.75)$, the same locations as those used in Zhang et al. (1995).

The boundary conditions are specified as follows. At the inlet boundary, a uniform flow velocity U is specified in the x-direction. At the outlet, the Neumann boundary condition (i.e., zero normal gradient) is applied for the velocity, and the pressure is specified as a reference value of zero. Symmetry boundary conditions are applied at the top and bottom boundaries, while periodic boundary conditions are employed at the two lateral

boundaries perpendicular to the cylinder axis. A non-slip boundary condition is applied on the surfaces of the main cylinder and near-wake wires.

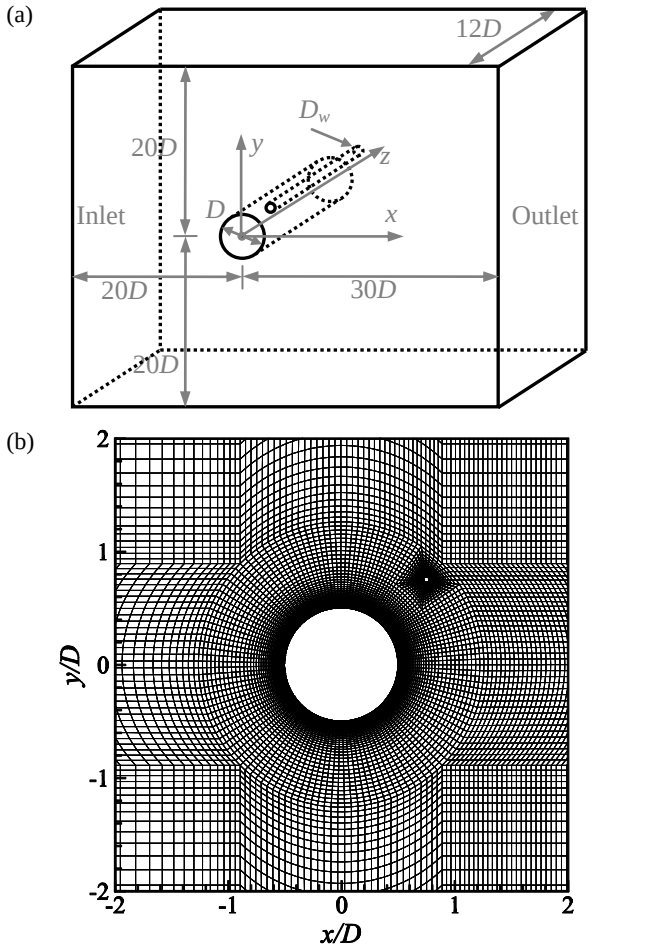

Figure 1. (a) Schematic model of the computational domain (not to scale) for the one-wire scenario, and (b) Close-up view of the 2D mesh near the main cylinder and wire for the one-wire scenario.

Computational Domain and Mesh

The computational domain and mesh for the one-wire scenario are reported below. A mesh dependence study is carried out for the one-wire scenario. For the two-wire scenario, the two near-wake wires and consequently the mesh are symmetrical about the wake centreline.

The two-dimensional (2D) mesh for the one-wire scenario (Figure 1(b)) is detailed as follows. The computational domain size in the *x*-*y* plane (i.e., the plane perpendicular to the cylinder span) is $50D \times 40D$. For the main cylinder, the cylinder perimeter is discretized with 142 nodes, and the radial size of the first layer of mesh next to the cylinder is $0.001D$. For the near-wake wire, the wire perimeter is discretized with 42 nodes, and the radial size of the first layer of mesh next to the wire is $0.0054D_w$. The non-dimensional wall distances (y^+) on the main cylinder and wire surfaces are less than 0.1 for all of the cases considered in this study (up to Re = 300). To capture detailed wake flow structures, a relatively high mesh resolution is used in the near-wake by specifying a streamwise mesh size varying linearly from $0.04D$ at x/D = 1 to $0.09D$ at x/D = 10.

The computational domain size and mesh resolution have been chosen based on a parameter dependence check. First, the adequacy of mesh resolution and domain size in the *x*-*y* plane was examined by a number of 2D simulations at Re = 300, the largest Re used in this study. It is found that by doubling the domain size in each direction or by doubling the cell number in both *x*- and *y*-directions, the variations of the hydrodynamic forces (including the Strouhal number, the time-averaged drag coefficient, and the root-mean-square lift coefficient) on the main cylinder and wire are all generally within 1%.

A 3D mesh was generated by replicating the 2D mesh along the *z*-axis, resulting in an identical mesh resolution in all planes perpendicular to the cylinder span. Based on Jiang et al. (2016) for flow past an isolated circular cylinder, the spanwise domain length (L_z) and spanwise cell size (Δz) for the present 3D mesh are specified as $12D$ and $0.1D$, respectively. It is found that by adopting an extended mesh (L_z is increased from $12D$ to $24D$) or a refined mesh (Δz is decreased from $0.1D$ to $0.05D$) at Re = 300, the Strouhal number and time-averaged drag coefficient for the fully developed 3D flow (with a sampling period of more than 800 non-dimensional time units which is defined as $t^* = Ut/D$) are both within 0.3%.

The above 2D and 3D mesh dependence studies demonstrate that the reported 3D mesh is adequate for the numerical simulations in the present study.

Numerical Results

Spatiotemporal Symmetry of the 2D Flow

It is well-known (see, e.g., Blackburn et al., 2005) that the 2D circular cylinder wake possesses a Z_2 spatiotemporal symmetry. In contrast, it is apparent that the one-wire scenario does not possess the Z_2 spatiotemporal symmetry since the wire is placed asymmetrical about the wake centreline, which forms a necessary condition for the emergence of Mode C instability. Figure. 2 shows the 2D vortex contours for the one-wire scenario at Re = 166 (just below the critical Re for the secondary instability of Re_{cr} = 166.4) with $T/2$ (T being the vortex shedding period) apart. The vortex contours are shown by the iso-surfaces of the spanwise vorticity ω_z, defined in a non-dimensional form of:

$$\omega_z = \left(\frac{\partial u_y}{\partial x} - \frac{\partial u_x}{\partial y} \right) \frac{D}{U} \tag{3}$$

As can be seen in Figure. 2, the Z_2 spatiotemporal symmetry of the 2D wake flow is broken by the placement of the wire in the near wake.

It is therefore interesting to examine the existence of the spatiotemporal symmetry in the wake of the two-wire scenario. Similarly, Figure. 3 shows the 2D vortex contours for the two-wire scenario at Re = 215 (just below Re_{cr} = 215.6) with $T/2$ apart. It is seen from Figure. 3 that the wake flow of the two-wire scenario does possess the Z_2 spatiotemporal symmetry. As a result, the Mode C wake instability is unlikely to occur under such a condition.

Wake Mode of the Secondary Instability

Subsequently, 3D DNS are used to predict the 3D wake instability mode, as well as the Re_{cr} value and the corresponding spanwise wavelength (λ_{cr}) of the 3D mode. The predicted neutral instability curves for the no-wire (i.e., an isolated cylinder), one-wire, and two-wire scenarios are shown in Figure. 4. The corresponding wake instability modes at Re slightly larger than Re_{cr} for the three scenarios are shown in Figure. 5. The wake modes are captured by the iso-surfaces of the streamwise vorticity ω_x, defined in a non-dimensional form of:

$$\omega_x = \left(\frac{\partial u_z}{\partial y} - \frac{\partial u_y}{\partial z} \right) \frac{D}{U} \tag{4}$$

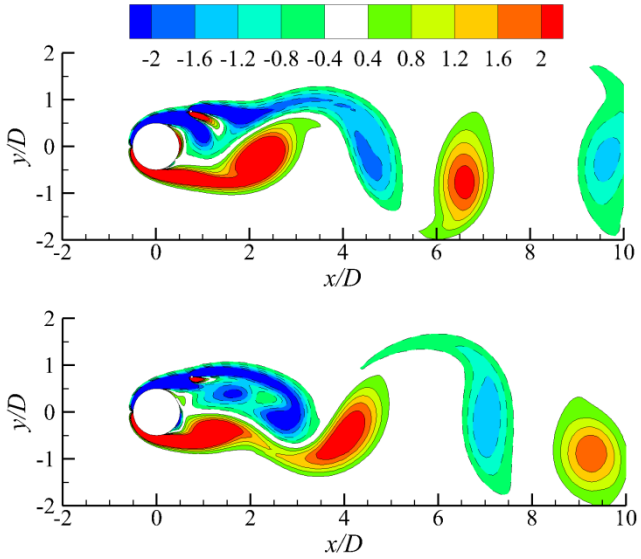

Figure. 2. 2D vortex contours for the one-wire scenario at Re = 166 (just below Re_{cr} = 166.4) with $T/2$ apart.

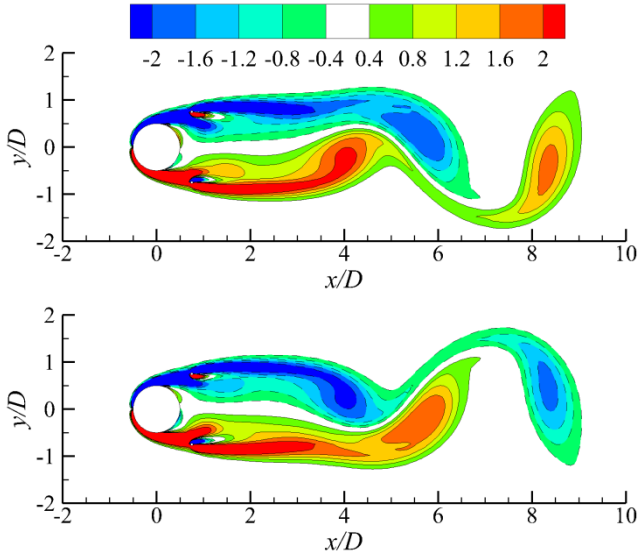

Figure. 3. 2D vortex contours for the two-wire scenario at Re = 215 (just below Re_{cr} = 215.6) with $T/2$ apart.

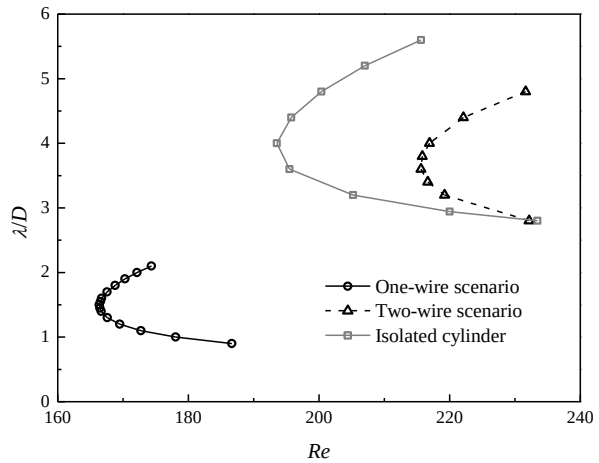

Figure. 4. Neutral instability curves for the case of an isolated cylinder (i.e., no-wire) and one-wire and two-wire scenarios.

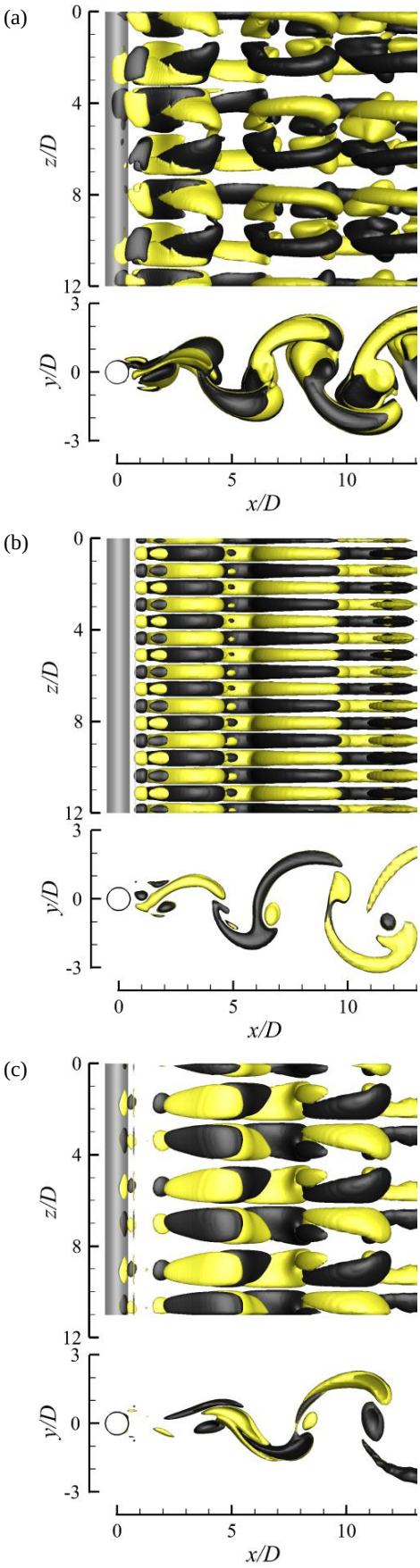

Figure. 5. Iso-surfaces of ω_x for (a) the case of an isolated cylinder at Re = 200 with ω_x = ±0.3, (b) the one-wire scenario at Re = 167 with ω_x = ±0.03, and (c) the two-wire scenario at Re = 220 with ω_x = ±0.1. Dark grey and light yellow denote positive and negative values, respectively. The flow is from the left to the right past the cylinder on the left.

For the case of an isolated cylinder, the secondary wake instability is represented by a Mode A instability (Figure. 5(a)) at (Re_{cr}, λ_{cr}) = (193.5, 4.0), which is in good agreement with the onset of Mode A at (Re_{cr}, λ_{cr}) = (190.2, 3.966) predicted by Posdziech and Grundmann (2001) through linear stability analysis.

For the one-wire scenario, the secondary instability is represented by a Mode C instability (Figure. 5(b)) at (Re_{cr}, λ_{cr}) = (166.4, 1.5) with the present setup of D_w/D = 0.05. Similarly, the Re_{cr} values for Mode C identified experimentally are Re_{cr} = 170 by Zhang et al. (1995) with D_w/D = 0.006, and Re_{cr} = 165 – 180 by Yildirim et al. (2013) with D_w/D = 0.01.

For the two-wire scenario, Zhang et al. (1995) reported a Mode C wake instability. However, as shown in Figure. 4 and Figure. 5(c), a secondary instability of Mode A is observed at (Re_{cr}, λ_{cr}) = (215.6, 3.6) in the present study. Together with the 2D vortex contours shown in Figure. 3 which display the Z_2 spatiotemporal symmetry, the present results support the finding by Blackburn and Sheard (2010) that the breaking of the Z_2 spatiotemporal symmetry of the 2D wake flow is a necessary condition for the emergence of Mode C wake instability. However, it should be noted that the Mode C instability does not occur unconditionally once the Z_2 spatiotemporal symmetry of the wake flow is broken. Rather, Mode C usually occurs when the wake flow is asymmetrical about the wake centreline to a large degree.

Conclusions

The secondary instabilities in the wake of a circular cylinder with near-wake wire disturbances are investigated in the present study by using 3D DNS. For the one-wire scenario with one wire placed asymmetrical about the wake centreline, the secondary instability is represented by a Mode C wake instability at (Re_{cr}, λ_{cr}) = (166.4, 1.5). In contrast, for the two-wire scenario with two wires placed symmetrical about the wake centreline, the secondary instability is represented by a Mode A wake instability at (Re_{cr}, λ_{cr}) = (215.6, 3.6), similar to the characteristics of Mode A for an isolated cylinder at (Re_{cr}, λ_{cr}) = (193.5, 4.0). Compared with the one-wire scenario, the existence of the Z_2 spatiotemporal symmetry in the 2D wake flow of the two-wire scenario is the reason why Mode C is suppressed in this case.

Acknowledgments

This work was supported by resources provided by the Pawsey Supercomputing Centre with funding from the Australian Government and the Government of Western Australia. The first author would like to acknowledge the support from the Australian Government and the University of Western Australia by providing IPRS and APA scholarships for a doctoral degree. The third author would like to acknowledge the support from the Australian Research Council through Discovery Early Career Research Award (DE150100428).

References

[1] Blackburn, H.M., Marques, F., Lopez, J.M., 2005. Symmetry breaking of two-dimensional time-periodic wakes. Journal of Fluid Mechanics 522, 395–411.

[2] Blackburn, H.M., Sheard, G.J., 2010. On quasiperiodic and subharmonic Floquet wake instabilities. Physics of Fluids 22, 031701.

[3] Carmo, B.S., Sherwin, S.J., Bearman, P.W., Willden, R.H.J., 2008. Wake transition in the flow around two circular cylinders in staggered arrangements. Journal of Fluid Mechanics 597, 1–29.

[4] Jiang, H., Cheng, L., Draper, S., An, H., Tong, F., 2016. Three-dimensional direct numerical simulation of wake transitions of a circular cylinder. Journal of Fluid Mechanics 801, 353–391.

[5] Posdziech, O., Grundmann, R., 2001. Numerical simulation of the flow around an infinitely long circular cylinder in the transition regime. Theoretical and Computational Fluid Dynamics 15, 121–141.

[6] Rao, A., Leontini, J., Thompson, M.C., Hourigan, K., 2013. Three-dimensionality in the wake of a rotating cylinder in a uniform flow. Journal of Fluid Mechanics 717, 1–29.

[7] Sheard, G.J., Thompson, M.C., Hourigan, K., 2003. From spheres to circular cylinders: the stability and flow structures of bluff ring wakes. Journal of Fluid Mechanics 492, 147–180.

[8] Sheard, G.J., Fitzgerald, M.J., Ryan, K., 2009. Cylinders with square cross-section: wake instabilities with incidence angle variation. Journal of Fluid Mechanics 630, 43–69.

[9] Williamson, C.H.K., 1996. Three-dimensional wake transition. Journal of Fluid Mechanics 328, 345–407.

[10] Yildirim, I., Rindt, C.C.M., van Steenhoven, A.A., 2013. Mode C flow transition behind a circular cylinder with a near-wake wire disturbance. Journal of Fluid Mechanics 727, 30–55.

[11] Zhang, H.Q., Fey, U., Noack, B.R., König, M., Eckelmann, H., 1995. On the transition of the cylinder wake. Physics of Fluids 7, 779.